

Point-contact study of gap amplitude and symmetry in $\text{RuSr}_2\text{GdCu}_2\text{O}_8$

G.A. Ummarino ^{††}, A. Calzolari [†], D. Daghero [†], R.S. Gonnelli [†], V.A. Stepanov [‡], R.Masini [§], M.R. Cimberle ^{||}

[†]INFM – Dipartimento di Fisica, Politecnico di Torino, 10129 Torino, Italy

[‡]P.N. Lebedev Physical Institute, Russian Academy of Sciences, 119991 Moscow, Russia

[§]CNR - IENI, Sezione di Milano, 20125, Milano, Italy

^{||} IMEM-CNR Sezione di Genova, 16146 Genova, Italy

Abstract. We present the results of point-contact spectroscopy measurements in polycrystalline $\text{RuSr}_2\text{GdCu}_2\text{O}_8$ samples previously characterized from both the structural and the electrical point of view. AC susceptibility and resistivity measurements, as well as SEM and optical microscopy, indicate that the polycrystalline material is made up of small, weakly connected grains. Possibly because of this morphology, point-contact measurements turned out to be rather difficult. Best reproducibility of the conductance curves was achieved in point contacts obtained by pressing Au or Pt-Ir tips on the surface of the samples. The low-temperature conductance curves reproducibly show a clear zero-bias cusp that might be interpreted as due to Andreev reflection at the normal metal-superconductor interface in the case where the superconducting order parameter has a pure d -wave symmetry - even though alternative explanations cannot be ruled out. In this paper we show that these curves can indeed be fitted, in the framework of the generalised BTK model, by using pure d -wave symmetry and a gap of the order of 6 meV. Finally, we present the temperature dependence of the conductance curves from 4.2 K up to the critical temperature of the junctions.

1. Introduction

The hybrid ruthenate-cuprate superconductor $\text{RuSr}_2\text{GdCu}_2\text{O}_8$ (Ru-1212) is a triple perovskite material comprising CuO_2 bilayers and RuO_2 monolayers. It was originally synthesized [1] with the purpose of incorporating a metallic layer between the CuO_2 planes, so as to enhance the inter-layer coupling and reduce the anisotropy. The role of the ruthenium-oxide layers was thus intended to be similar to that of the one-dimensional Cu-O chains in YBCO. In these layers, the ruthenium atoms present the same square-planar coordination as in the CuO_2 planes, with a similar bond length. As evidence by X-ray absorption near edge structure (XANES) [2], nuclear magnetic resonance (NMR) [3, 4] and magnetization measurements [5] ruthenium occurs in a mixed valence state as Ru^{4+} and Ru^{5+} with concentrations equal to 40% and 60% respectively. As a result, RuO_2 planes also act as a charge reservoir, doping the superconducting CuO_2 planes.

In addition to the superconducting transition, the compound features magnetic order below the temperature $T_M \simeq 133$ K, whose nature is still controversial. After the first results suggesting a ferromagnetic order [6, 7] some theoretical and experimental arguments have been reported in favour of an antiferromagnetic ordering [8, 9]. One possibility to reconcile

[†] To whom correspondence should be addressed (giovanni.ummarino@infm.polito.it)

these opposite evidences is to admit that the ferromagnetically-ordered RuO_2 planes are coupled to one another via an antiferromagnetic interaction [5].

Whatever its nature, the magnetic order is found to survive even when superconductivity sets in. While the coexistence of antiferromagnetism and superconductivity is common among cuprates, the coexistence of superconductivity and ferromagnetism would contrast the widespread belief that these two ordering are competing and mutually exclusive. This is the more true if one takes into account that, according to muon-spin rotation (μSR) measurements [6], the ferromagnetic order looks uniform and homogeneous, even below T_c , on a scale of typically 20\AA . This would imply that the interaction between the superconducting and the ferromagnetic order parameter is very weak. As a matter of fact, high-temperature susceptibility data indicate that the ferromagnetic order involves only the Ru moments [6] while Zn substitutions suggest that only the CuO_2 planes host the superconducting charge carriers [6]. The decoupling of CuO_2 and RuO_2 layers has been recently confirmed by a comprehensive study of DC and AC susceptibility, DC resistance, magnetoresistance, Hall effect and microwave absorption [10], showing that the RuO_2 planes are conducting but do not develop superconductivity.

In spite of the great experimental and theoretical efforts focused on the interplay between superconductivity and magnetism, to our knowledge no spectroscopic studies of the superconducting order parameter in $\text{RuSr}_2\text{GdCu}_2\text{O}_8$ have been reported so far in literature. In this paper we present and discuss the results of point-contact spectroscopy measurements in polycrystalline $\text{RuSr}_2\text{GdCu}_2\text{O}_8$ previously characterized by SEM and optical microscopy, AC susceptibility and resistivity measurements. We will show that the order-parameter symmetry that best fits the experimental conductance curves is d -wave, thus indicating that, as in the other cuprates, superconductivity in Ru-1212 is due to singlet Cooper pairs.

2. Experimental details

2.1. Preparation and characterization of the samples

The single-phase, polycrystalline samples we used for our measurements were synthesized by solid state reaction starting from high purity stoichiometric powders of RuO_2 , Gd_2O_3 , CuO and SrCO_3 . The raw materials were reacted in air at about $960\text{ }^\circ\text{C}$, in order to decompose the SrCO_3 . Then, they were heated in N_2 flow at $1010\text{ }^\circ\text{C}$ and annealed in O_2 flow at temperatures ranging from 1050 to $1060\text{ }^\circ\text{C}$. Finally, a prolonged anneal in flowing O_2 at $1060\text{ }^\circ\text{C}$ was performed, during which the material densifies, granularity is reduced and ordering within the crystal structure develops. For further details on the preparation technique see Ref.[11].

Figure 1 reports a SEM image of one of the samples studied. It is clearly seen that the thermal treatment [11] ensures a partial sinterization (some grains begins to coalesce in big aggregates) but a matrix of weakly connected grains is still present. This kind of aggregation can be also perceived by optical inspections with AFM.

Previous to point-contact fabrication and PCS measurements, we quickly characterized the samples from the superconducting and electrical point of view, by means of resistivity and AC susceptibility measurements. Figure 2a reports the temperature dependence of the real and imaginary parts of the susceptibility, measured in the absence of DC magnetic field. The measurements were carried out in a home-made susceptometer designed to allow measurements also in very small samples (sub-mm size). The temperature is given by a SMD-type resistor mounted in the close proximity of the coil containing the sample. Unfortunately, it is calibrated only up to 130 K so that the peak in χ' at about 130 K is only partly visible. The correction for the demagnetizing factor and the correct volume are taken into account in

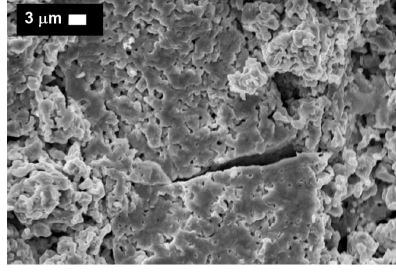


Figure 1. SEM image of a polycrystalline $\text{RuSr}_2\text{GdCu}_2\text{O}_8$ sample similar to that used for our measurements, and synthesized in Genoa (from Ref. [11]).

the conversion from the imbalance voltage to the susceptibility. It is clear that, in this kind of measurements, what we actually observe is the volume fraction that is diamagnetically shielded, and *not* the superconducting fraction. In this sense, we can safely say that in our samples the superconducting volume is *at most* 80% of the total volume (see Figure 2a). The diamagnetic transition sets on at $T_c^{dia} \simeq 27$ K, while the middle point T_c^{mid} (the maximum peak in the imaginary part curves) is estimated at $T_c^{mid} \simeq 23.4$ K.

The resistivity measurements were carried out by using the conventional four-probe technique and by using AC current to cancel out thermoelectric effects. The voltage signal was recorded by using a EG&G lock-in amplifier that allows using very small frequencies. In particular, the $\rho(T)$ curve reported in Figure 2b was obtained with a very small current intensity (3 mA p-p) to reduce possible heating effects, with a frequency of 3.0 Hz. The curve witnesses the good quality of the samples. It is well known that the physical properties of this rutheno-cuprate material – and in particular its critical temperature – are strongly dependent on the details of the preparation procedure. In the present case, the temperature at which the resistance goes to zero ($T_c^0 = 26$ K) is rather high if compared to other data from literature. The transition sets on at $T_c^{onset} = 45$ K, so that $\Delta T_c = 19$ K is the transition width. The change in slope usually attributed to the onset of the magnetic order at T_M is also shown.

2.2. Point-contact measurements

Due to the granularity of the material and its only partial sinterization, the surface of the samples looked rather rough and brittle. As a result, point-contact measurements turned out to be rather difficult. We tried with tips of different materials (Au, Pt, Pt-Ir and so on), made by electrochemical etching (with a 25% HNO_3 + 75% HCl solution) starting from wires of different thickness. We also tried to use, instead of the tip, Ag paste or In flakes to make the contacts. In the end, we achieved the best reproducibility of the conductance curves in point contacts obtained by using tips (of either Au or Pt-Ir) made by starting from thick wires ($\varnothing \leq 0.1$ mm), that could apply a rather large pressure on the sample. In these contacts, we were able to follow the temperature evolution of the conductance curves, from 4.2 K up to the critical temperature of the junction.

Once established the contact between tip and sample, we measured the DC $I - V$ characteristic of the contact and then numerically calculated the differential conductance, i.e. the first derivative dI/dV as a function of the voltage bias V . To allow the comparison to theoretical models, the resulting curves were then normalized to the normal-state conductance. Figure 3a reports some examples of normalized conductance curves measured at low

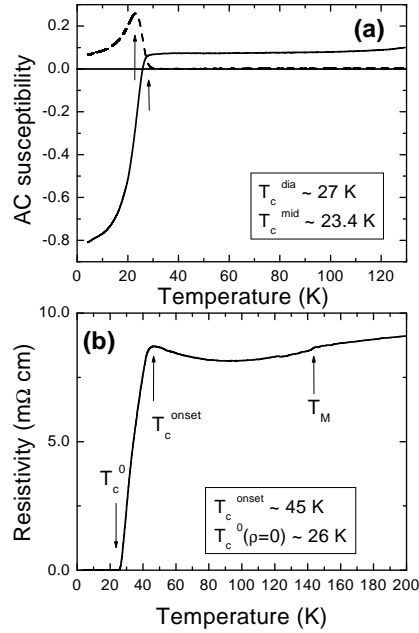


Figure 2. (a) An example of AC susceptibility transition of a $\text{RuSr}_2\text{GdCu}_2\text{O}_8$ sample. The values of the relevant critical temperatures are also reported. (b) Resistivity vs. temperature for one of our samples. The relevant temperatures corresponding to the magnetic and superconducting transitions are also indicated.

temperature ($T = 4.2$ K). The curves are vertically shifted for clarity. All of them feature a zero-bias conductance peak (ZBCP), and more or less pronounced shoulders at finite voltage. The zero-bias peak is very similar to that produced by Andreev reflection in normal metal/ d -wave superconductor junctions, when the positive interference between incoming and reflected electron gives rise to the zero-energy Andreev bound states. Therefore, the presence of a ZBCP is suggestive of a d -wave order parameter in Ru-1212.

To investigate in more detail this possibility, we tried to fit the low-temperature normalized conductance curves by using the Blonder-Tinkham-Klapwijk model [12] generalized to non-conventional order parameter symmetries [13]. For the time being, we only considered the simplest possible symmetries: d -wave (because of the analogy with other cuprates) and p -wave (suggested by the comparison with the superconducting ruthenate Sr_2RuO_4). In Figure 3b an experimental conductance curve (symbols) is reported together with the best-fitting curves obtained with pure d -wave (solid line) and pure p -wave (dashed line) order parameter symmetry. The values of the best-fitting parameters are also reported in the legend.

In the case of the d -wave fit, the free parameters are: the maximum gap amplitude Δ , the barrier transparency parameter Z (which is proportional to the potential barrier height at the interface) and the angle α the direction of current injection makes with the normal to the interface. In addition to these parameters, a phenomenological broadening parameter Γ was needed, that mimics pair-breaking effects due, for example, to non-magnetic impurities. Notice that, however, Γ is much smaller than the gap amplitude ($\Delta_d = 6.0$ meV) given by the fit.

As far as the p -wave symmetry is concerned, we chose one of the triplet p -wave pair potential symmetries (the so-called E_u states) proposed by Machida *et al* [14] and by Sgrist

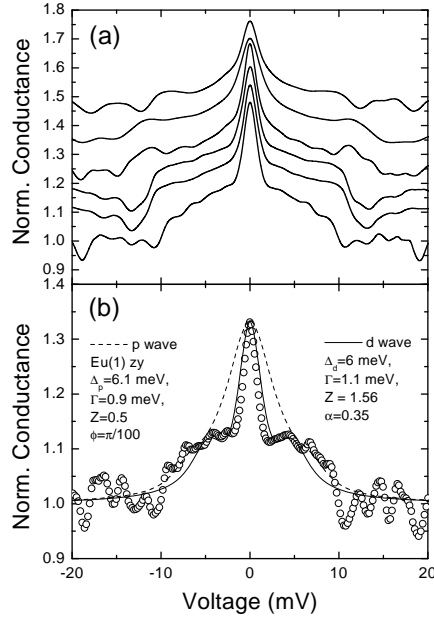


Figure 3. (a) normalized conductance curves obtained by PCS with Pt-Ir tips at low temperature. (b) an example of normalized conductance curve fitted with a pure d -wave symmetry or with a pure p -wave symmetry. The best fit was due to the pure d -wave order parameter symmetry.

and Zhitomirsky [15]. The free fitting parameters are: the gap amplitude Δ , the barrier parameter Z , the azimuthal angle ϕ and, as in the previous case, the broadening parameter Γ . Interestingly, the amplitude of the p -wave gap obtained from the fit ($\Delta_p = 6.1$ meV) is consistent with that obtained with the d -wave symmetry.

It is clearly seen in Figure 3b that the d -wave fit works much better than the p -wave one. In particular, the d -wave curve accounts for both the height and the width of the zero-bias conductance peak, and also follows rather well the shoulders at finite energy. On the contrary, the p -wave curve has a smoother bell-shaped behaviour that cannot reproduce the main features of the experimental conductance curve. Thus, the d -wave symmetry is much more compatible with our findings. This fact indicates that the nature of superconductivity in the Ru-1212 compound is by far more similar to other cuprates than to ruthenates. In fact: i) the d -wave symmetry is common among cuprates, for example in BSCCO; ii) if the order parameter is d -wave, the Cooper pairs turn out to be spin singlets as in conventional superconductors and HTSC, and not exotic spin-triplet states as in Sr_2RuO_4 . Indirectly, this similarity with other cuprates supports the evidences of a confinement of superconductivity on the CuO_2 layers (that are common to Ru-1212 and copper oxides), with no contribution from the Ru-O sublattice [10].

When the junction was sufficiently stable, we could follow the evolution of its conductance curves on heating, from 4.2 K up to the critical temperature of the junction, where the Andreev-reflection features disappear. Figure 4 reports two examples of temperature dependence of the normalized conductance curves. The curves are vertically shifted for clarity and ordered for increasing values of the temperature. Superimposed to the experimental data (symbols) we also show the best-fitting d -wave symmetry curves. It is clear that, in general, the fit is satisfactory. In these few cases where the agreement between theoretical and

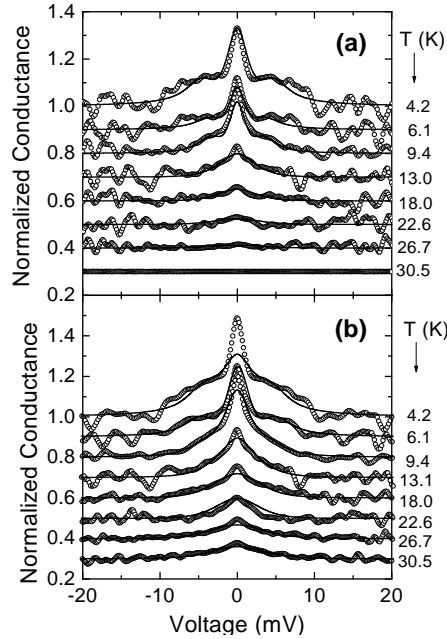


Figure 4. Temperature dependence of the conductance curves of point-contacts obtained by using a Pt-Ir and a Au tip, respectively. The diameter of the starting wires in which the tips were made by electrochemical process was $\varnothing = 0.1$ and $\varnothing = 0.125$ mm, respectively. The temperature corresponding to each curve is reported on the right side of the panel. The experimental conductance curves (symbols) are compared to the theoretical best-fitting BTK curves, calculated for a d -wave order parameter.

experimental data is poor (see, for example, the upper curve in panel (b)) the choice had to be made between the theoretical curve that best fits the ZBCP and the one that, instead, follows the shoulders.

It is clearly seen that, in both cases, the thermal evolution of the conductance curves is approximately the same, with a progressive decrease of the finite-voltage shoulders and of the zero-bias peak. As a matter of fact, also the behaviour of the best-fit parameters as a function of the temperature is very similar in the two cases. First of all, the broadening parameter Γ decreases quickly and goes to zero well before the critical temperature. Second, the gap amplitude starts decreasing at low temperature, contrary to what expected in the conventional BCS theory, and goes to zero at T_c in a sub-linear way. Figure 5 reports the complete $\Delta(T)$ curve for the conductances of Figure 4a, that are better fitted by the model. In the other case, the behaviour is similar but the gap values are slightly greater at intermediate temperatures.

3. Conclusions

In conclusion, we have presented some preliminary results of point-contact spectroscopy in the hybrid ruthenate-cuprate superconductor $\text{RuSr}_2\text{GdCu}_2\text{O}_8$. The low temperature (4.2 K) conductance curves present a clear zero-bias conductance peak, that decreases and goes to zero at the increase of the temperature. The experimental conductance curves turn out to be compatible with a pure d -wave symmetry of the order parameter, which suggests a tighter similarity of this compound to the other cuprates rather than to the ruthenate Sr_2RuO_4 . It is worth reminding that, however, alternative explanations cannot be ruled out, due to the

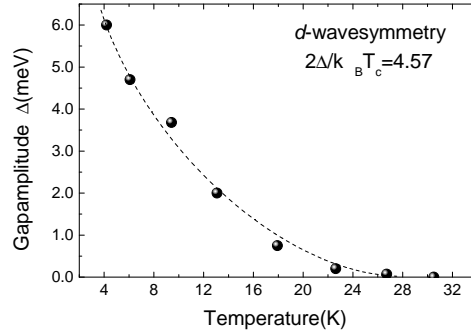


Figure 5. Superconducting gap values as a function of the temperature, as obtained from the generalized BTK fit of the experimental data in Figure 4a. The line is only a guide to the eye.

complexity of the material under study and in particular to its magnetic properties.

One of the authors (V.A.S.) acknowledges the support from RFBR (project N. 02-02-17133) and the Ministry of Science and Technologies of the Russian Federation (contract N. 40.012.1.1.1357).

References

- [1] Bauernfeind L, Widder W and Braun H F 1995 *Physica C* textbf254 151; Bauernfeind L, Widder W and Braun H F 1996 *J. Low Temp. Phys.* **105** 1605.
- [2] Liu R S, Jang L -Y, Hung H -H and Tallon J L 2001 *Phys. Rev. B* **63** 212507.
- [3] Kumagai K, Takada S and Furukawa Y 2001 *Phys. Rev. B* **63** 180509.
- [4] Tokunaga Y, Kotegawa H, Ishida K, Kitaoka Y, Takagiwa H and Akimitsu J 2001 *Phys. Rev. Lett.* **86** 5767.
- [5] Butera A, Fainstein A, Winkler E and Tallon J L 2001 *Phys. Rev. B* **63** 054442.
- [6] Bernhard C, Tallon J L, Niedermayer Ch, Blasius Th, Golnik A, Brücher E, Kremer R K, Noakes D R, Stronach C E and Ansaldo E J 1999 *Phys. Rev. B* **59** 21 14099.
- [7] McCrone J E, Cooper J R and Tallon J L 1999 *J. Low Temp. Phys.* **117** 1199.
- [8] Lynn J W, Keimer B, Ulrich C, Bernhard C and Tallon J L 2000 *Phys. Rev. B* **61** R14964.
- [9] Nakamura K, Park K T, Freeman A J, and Jorgensen J D 2000 *Phys. Rev. B* **63** 024507.
- [10] Požek M, Dulčić A, Paar D, Hamzić A, Basletić M, Tafra E, Williams G V M and Krämer S 2002 *Phys. Rev. B* **65** 174514.
- [11] Masini M, Artini C, Cimberle M R, Costa G A, Carnasciali M and Ferretti M 2001 *Ruthenate and ruthenocuprate materials: theory and experiments* (Vietri). To be published on LNP Series, Springer Verlag, Berlin, Noce C, Vecchione A, Cuoco M and Romano A Eds 2002.
- [12] Blonder G E, Tinkham M and Klapwijk T M 1982 *Phys. Rev. B* **25** 4515.
- [13] Kashiwaya S and Tanaka Y 2000 *Rep. Prog. Phys.* **63** 1641; Yamashiro M, Tanaka Y and Kashiwaya S 1997 *Phys. Rev. B* **56** 7847.
- [14] Machida K, Ozaki M and Ohmi T, 1996 *J. Phys. Soc. Jpn.* **65** 3720.
- [15] Sigrist M and Zhitomirsky 1996 *J. Phys. Soc. Jpn.* **65** 3452.